nature materials

ARTICLES

PUBLISHED ONLINE: 13 OCTOBER 2013 | DOI: 10.1038/NMAT3766

In situ cell manipulation through enzymatic hydrogel photopatterning

Katarzyna A. Mosiewicz[1†], Laura Kolb[1†], André J. van der Vlies[1,2], Mikaël M. Martino[1,3], Philipp S. Lienemann[4], Jeffrey A. Hubbell[1], Martin Ehrbar[4] and Matthias P. Lutolf[1*]

The physicochemical properties of hydrogels can be manipulated in both space and time through the controlled application of a light beam. However, methods for hydrogel photopatterning either fail to maintain the bioactivity of fragile proteins and are thus limited to short peptides, or have been used in hydrogels that often do not support three-dimensional (3D) cell growth. Here, we show that the 3D invasion of primary human mesenchymal stem cells can be spatiotemporally controlled by micropatterning the hydrogel with desired extracellular matrix (ECM) proteins and growth factors. A peptide substrate of activated transglutaminase factor XIII (FXIIIa)—a key ECM crosslinking enzyme—is rendered photosensitive by masking its active site with a photolabile cage group. Covalent incorporation of the caged FXIIIa substrate into poly(ethylene glycol) hydrogels and subsequent laser-scanning lithography affords highly localized biomolecule tethering. This approach for the 3D manipulation of cells within gels should open up avenues for the study and manipulation of cell signalling.

Synthetic hydrogels have been engineered as powerful scaffolds to mimic a cell's native microenvironment to rationally control cellular behaviour in tissue engineering[1,2]. The application of such artificial ECMs (aECMs), and in particular their fabrication with well-defined physicochemical bulk properties, has also enabled researchers to gain insights into the biology of crosstalk between cells and microenvironmental components (for example, refs 3–5). However, the control over bulk gel properties is often not sufficient to elicit a desired morphogenetic response and to ultimately form a functional tissue *de novo*. In the absence of tightly orchestrated and localized morphogenetic cellular stimuli within aECMs, multicellular processes necessary for tissue formation cannot easily be induced[6]. In contrast to their engineered counterparts, natural ECMs are not homogeneous entities but rather spatially patterned milieus with a cell-type specific composition and structure that can rapidly change over time in response to the physiological demands of a tissue. For example, tissue or organ formation starts with a spatiotemporally coordinated cell polarization, and during tissue regeneration the ECM is rapidly remodelled in a highly localized and heterogeneous manner. Therefore, biomimicry strategies in tissue engineering could benefit from precise control over aECM properties in space and in time.

To this end, important progress has been made over the past few years in the design of synthetic hydrogels with biochemical and biophysical properties that can be modulated by a light beam at the micrometre scale and at a desired time during an experiment[7]. Two complementary strategies have emerged. In one approach, dynamic changes in gel properties were achieved by locally cleaving photosensitive bonds to release biochemical ligands or decrease gel crosslinking density[8–10]. This strategy was, for example, used to influence the growth of encapsulated mesenchymal progenitor cells within photopolymerized poly(ethylene glycol) (PEG) hydrogels[8]. Photodegradation thus altered gel features in a subtractive manner rather than by addition of biological signals. Whereas native microenvironments are frequently degraded and remodelled by cellular activity (for example, during proteolysis in wound healing), locally modular microenvironments may emerge most frequently from the secretion of biological signals from a cellular source (for example, gradients of morphogens in embryonic development). Thus, as a second approach, this additive mode of local microenvironmental patterning was achieved by other groups using chemical crosslinking strategies[11–15]. Indeed, approaches employing radical reactions of acrylates or thiol-enes, or photoprotected thiol residues in Michael-type addition, have demonstrated successful local patterning of hydrogel matrices with simple cell-adhesion peptides[11,12,14].

These advances are exciting. Yet, in contrast to the relatively easy functionalization of gels with peptides, with one notable exception exploiting physical binding interactions[15], the patterning of more complex and physiologically relevant signalling proteins has not been achieved. This is not surprising, because the activity and stability of proteins can be compromised by bioconjugation reactions that are not sufficiently mild and specific. Moreover, full-length proteins cannot be easily modified with photosensitive moieties used in existing photopatterning techniques. We consequently reasoned that enzymatic crosslinking reactions might be ideal targets for spatiotemporally controlled *in situ* hydrogel patterning with fragile biomolecules such as proteins. We reasoned that by masking an enzymatic peptide substrate with a photolabile cage[16], the enzyme-mediated bioconjugation could be spatiotemporally controlled by light exposure according to the concept shown in Fig. 1. By covalently incorporating these caged substrates into a hydrogel network (Fig. 1a), subsequent local photoactivation (Fig. 1b) was expected to enable highly localized enzymatic biomolecule tethering (Fig. 1c). Here we show that this concept can be successfully reduced to practice, affording exquisite control

[1]Institute of Bioengineering, Ecole Polytechnique Fédérale de Lausanne (EPFL), CH-1015 Lausanne, Switzerland, [2]Division of Applied Chemistry, Graduate School of Engineering, Osaka University, Osaka 565-0871, Japan, [3]WPI Immunology Frontier Research Center (IFReC), Osaka University, Osaka 565-0871, Japan, [4]Department of Obstetrics, University of Zurich Hospital, CH-8091 Zurich, Switzerland. †These authors contributed equally to this work.
*e-mail: matthias.lutolf@epfl.ch

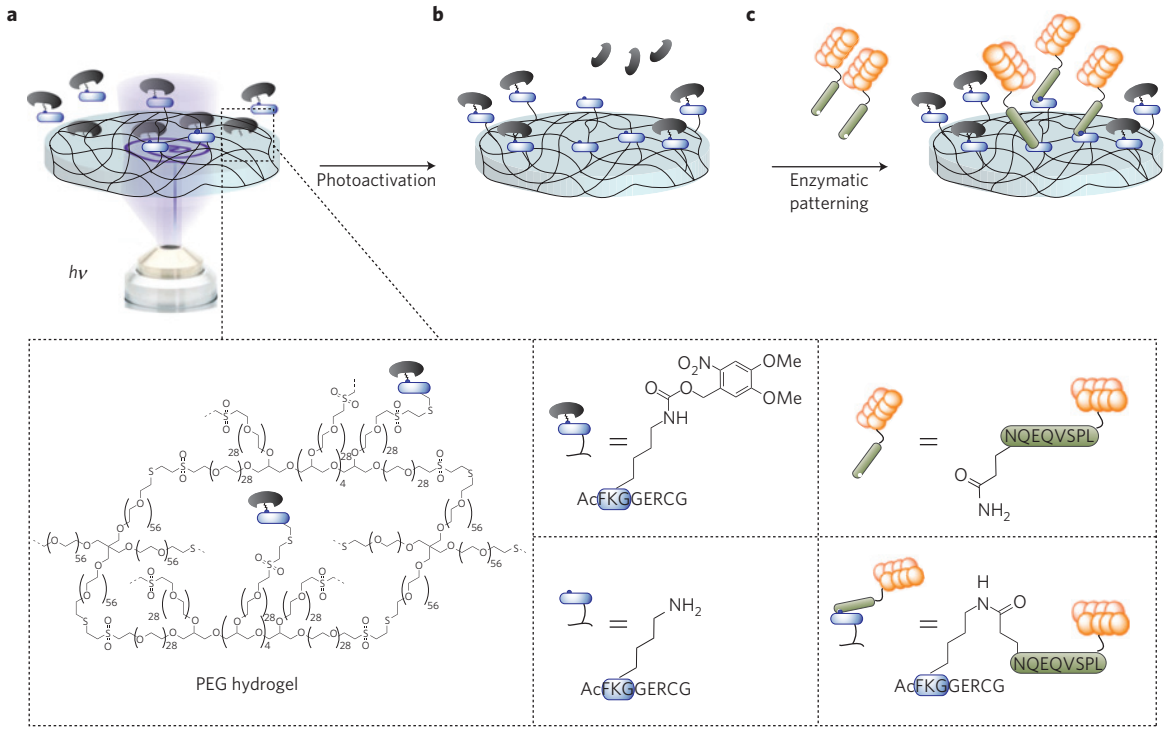

Figure 1 | Concept of light-controlled enzymatic biomolecule patterning of hydrogels. a, A photolabile, caged, and therefore inactive enzymatic peptide substrate is covalently incorporated into PEG hydrogels and can be activated by light. **b**, Localized cleavage of the cage by controlled light exposure from a confocal laser allows reactivation of the enzyme substrate. **c**, Enzyme-catalysed (here: the transglutaminase factor XIII) reaction of the uncaged substrate with a counter-reactive substrate on a biomolecule of interest allows covalent biomolecule tethering in a highly localized, user-defined pattern.

over the site-specific immobilization of virtually any desired protein within a synthetic hydrogel network.

We chose a crosslinking scheme catalysed by FXIIIa, a key enzyme responsible for fibrin polymerization during blood coagulation[17,18], because we, inspired by pioneering work of other groups on transglutaminase-mediated crosslinking of PEG hydrogels[19,20], had previously used FXIIIa for hydrogel crosslinking and biomolecule functionalization[21]. FXIIIa catalyses reactions between an ε-amine of lysine (K) onto a γ-carboxamide residue of glutamine (Q), resulting in the covalent bond formation of an ε-(γ-glutamyl)lysine isopeptide. To spatiotemporally control FXIIIa-mediated crosslinking, we abolished the enzymatic susceptibility of one of its substrates by covalent attachment of a photolabile cage that can be reactivated after photo-illumination (Fig. 1). The short amine donor FXIIIa substrate AcF**K**G, simply termed here as K-peptide, was chosen for the modification with the cage. The cage on the ε-amine of its lysine (K) was targeted to block the FXIIIa-mediated nucleophilic attack on the glutaminyl residue (Q) of the amine-acceptor peptide N**Q**EQVSPL (termed Q-peptide). As a photosensitive caging group, we chose nitroveratryloxycarbonyl (Nvoc) to modify lysine-Fmoc (Supplementary Fig. S1). In comparison with other cages that are active at lower excitation wavelengths, Nvoc has a broad absorption in ultraviolet/visible around 350 nm, which is advantageous in terms of a wider depth of uncaging penetration in tissues as well as reduced DNA and biomolecule damage[16,22]. Thus, we reasoned that this approach would be suitable for gel applications in the presence of cells *in vitro* and *in vivo*. The photoprotection of the ε-amine residue of the K-peptide was achieved by incorporation of a photoprotected lysine derivative during solid-phase peptide synthesis as described in the Supplementary Information.

We first assessed the feasibility of light-controlled enzymatic crosslinking by way of using a soluble model system (Fig. 2). When tested on high-pressure reverse-phase high-performance liquid chromatography (RP-HPLC) with an analytical C_{18}-column, the caged lysine-containing peptide [1′] was shown to elute at a different retention time (t_R) from the unmodified substrate [1] (Fig. 2a). Notably, two peaks corresponding to the caged product appeared after peptide purification performed by a semi-preparative C_{18}-column. As both peaks corresponded to the same mass (Supplementary Fig. S2) and had similar ultraviolet spectra (210–400 nm; Supplementary Fig. S3), it is very likely that they represent a different conformation of the same peptide. Importantly, when the caged peptide in solution was exposed to ultraviolet light from a mercury lamp, a new product was observed, corresponding to the unprotected FXIIIa substrate [1]. A variation of exposure times allowed us to quantify uncaging efficiencies by HPLC (Fig. 2a, inset). Accordingly, photolysis proceeded with first-order kinetics until a plateau was reached near completion after about 20 s (Fig. 2a, inset). The half-life of photolysis was calculated by linear regression to be $t_{1/2} = 10.5$ s (Supplementary Fig. S4).

To investigate FXIIIa-mediated crosslinking after uncaging, we incubated the caged K-peptide [1′] together with the counter-reactive Q-peptide [2] and FXIIIa to induce crosslinking (Fig. 2b). As expected, analytical HPLC analysis clearly indicated that the caged substrate was unable to undergo crosslinking, which occurred with unmodified substrate at $t_R = 7.7$ min. However, light exposure of the caged K-peptide [1′] in the presence of equimolar amounts of Q-peptide [2] and FXIIIa resulted in the crosslinked product [3] ($t_R = 9.5$ min), providing important first evidence for light-activated, enzymatic bond formation in this soluble model system.

In a next set of experiments we tested the light-triggered enzymatic functionalization of a synthetic hydrogel with a fluorescently labelled model Q-peptide (Fig. 3). The caged substrate was covalently incorporated into PEG networks by Michael-type addition of cysteine at the C terminus of the peptide with vinylsulphone groups on PEG macromers[23]. A confocal laser scanning microscope, equipped with a software-controlled positioning system of

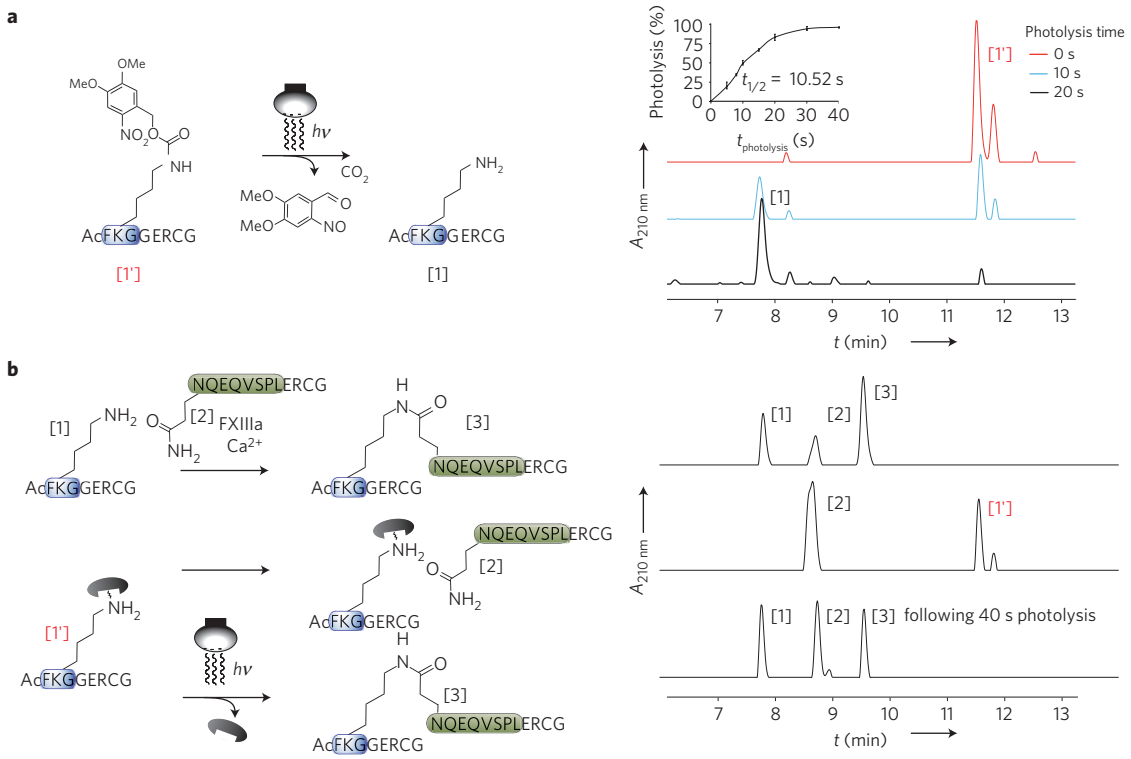

Figure 2 | Proof-of-principle of light-controlled enzymatic reactions using a soluble model system. a, Photolysis of the caged K-peptide substrate [1′] by exposure to light from an ultraviolet mercury lamp followed by HPLC analyses of the generated products. Calculated half-lives of uncaging ($t_{1/2}$; inset, right panel). **b**, HPLC analyses of FXIIIa-catalysed reactions in the presence of its counter-reactive substrate. Wild-type Q-peptide [2] crosslinked with K-peptide forms product [3] (positive control), whereas in the case of the caged K-peptide [1′] no crosslinking is detected. In contrast, exposure of the caged substrate [1′] to an ultraviolet mercury lamp results in complete photolysis (disappearance of [1′]) and reactivation of the FXIIIa-catalysed crosslinking reaction (isopeptide product [3]), proving that the concept outlined in Fig. 1 can be implemented.

an ultraviolet laser (405 nm), was used to create custom-made, spatially defined regions of interest (ROIs) of laser illumination. In the laser-exposed areas, the photolabile group was released to render the newly uncaged ε-amine group susceptible to FXIIIa-mediated crosslinking (Fig. 3a). Interestingly, the release of the cage could be followed *in situ* by confocal microscopy (Supplementary Fig. S5), a phenomenon that could be exploited to determine the efficiency of photolysis. To allow site-selective bioconjugation, the hydrogel films were immersed in a solution containing FXIIIa and the fluorescently labelled model Q-peptide. After washing, micrometre-scale fluorescent patterns of very high spatial fidelity were clearly visible (Fig. 3b). The patterns were detectable through the entire thickness of the thin hydrogel layer; that is, patterning occurs in three dimensions and not just on the gel surface (Supplementary Fig. S6). Of note, FXIII-mediated patterning can also be performed in the presence of serum, albeit with lower efficiency (Supplementary Fig. S7). Software-controlled positioning of the laser-beam enabled the patterning of any shape. Moreover, the discrete change of laser intensities in the form of aligned adjacent rectangular ROIs of interest allowed the generation of user-defined biomolecule gradients within hydrogels, in either a step-wise (Fig. 3c) or a continuous (Fig. 3d) fashion.

We next sought to demonstrate the applicability of our approach to pattern biomolecules within gels by way of a biologically relevant example, namely the morphogen vascular endothelial growth factor 121 ($VEGF_{121}$; Fig. 3e, left panel) and the recombinant fibronectin type III repeat 9–10 fragment of fibronectin[24] (FN_{9-10}; Supplementary Fig. S8). Indeed, because the activity and stability of proteins can be easily compromised by crosslinking reactions that are not highly site-specific, most previous approaches in hydrogel photopatterning by biomolecules were limited to short oligopeptides such as the minimal integrin-binding ligand RGD (refs 11,12,14). These signals can be readily modified to have photoreactive groups, which is not the case for full-length proteins. We used recombinant $VEGF_{121}$ engineered with an exogenous Q-peptide domain at the N terminus to enable enzymatic crosslinking[25]. On localized uncaging of the tethered caged K-peptide, hydrogel films were immersed in FXIIIa-containing buffer together with $VEGF_{121}$. Visualization of laser-patterned areas by immunostaining showed clearly visible and specific $VEGF_{121}$ patterns of high fidelity (Fig. 3e).

To determine whether the bioactivity of $VEGF_{121}$ could be altered on FXIIIa-mediated tethering to PEG, we used PEG-conjugated $VEGF_{121}$ as a soluble model system. To this end, $VEGF_{121}$ was modified with PEG monomethyl ether (mPEG; 5 kDa) either through site-specific catalysis, or through nonspecific chemical crosslinking using an amine-reactive mPEG succinimidyl ester (Supplementary Fig. S9). Using a HUVEC proliferation assay[25], we compared the mitogenic activity of both PEG–$VEGF_{121}$ constructs to native $VEGF_{121}$. At a relatively low (that is, non-saturating) concentration of 5 ng ml^{-1}, a significant reduction in the activity was found for nonspecifically coupled PEG–$VEGF_{121}$, in contrast to the site-specifically modified version (Supplementary Fig. S10), although the bioactivity of the two PEGylated proteins was not found to be statistically significant. Nevertheless, these data indeed suggest a good preservation of bioactivity for the FXIIIa-mediated tethering of proteins in our PEG hydrogel system.

We next used an enzyme-linked immunosorbent assay to determine the overall concentration of covalently incorporated $VEGF_{121}$ in matrix metalloproteinase (MMP)-sensitive PEG hydrogels[23] containing 1 mM K-peptide (see Supplementary Information for experimental details). FXIIIa-mediated tethering of 20 ng ml^{-1} (1.25 nM)

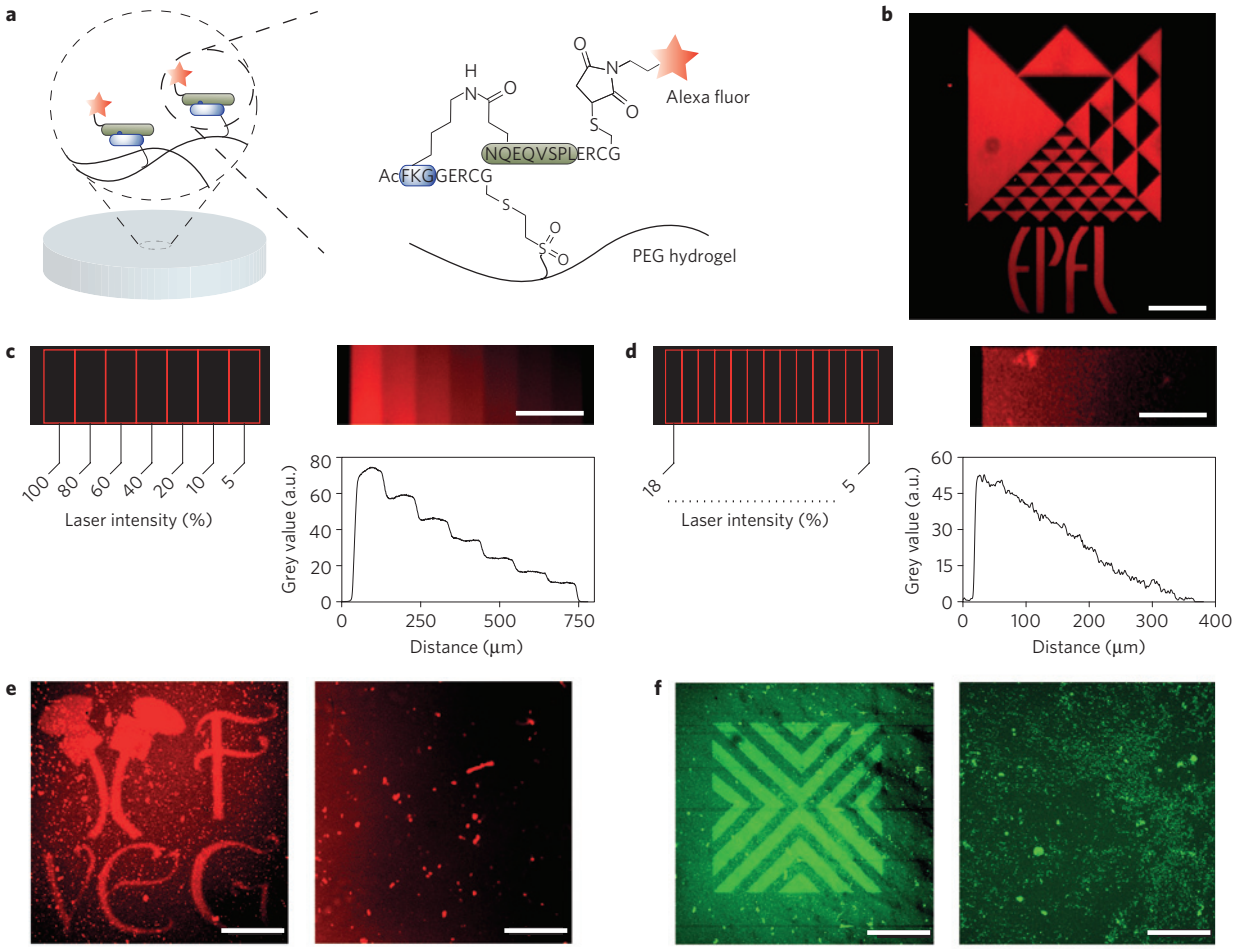

Figure 3 | Spatial patterning of hydrogels with fluorescently labelled model ligands and proteins. a, Photoactivation by laser scanning microscopy within designed ROIs and FXIIIa-catalysed attachment of a fluorescent model ligand. **b**, The laser-scanning technique allows the generation of precisely defined patterns of any arbitrary shape (scale bar, 200 μm). **c**, Step-wise biochemical gradients were obtained by titrating the laser intensity in each ROI (design: 7 × 100 μm-wide rectangular ROIs, left panel, scale bar, 200 μm). **d**, Continuous gradients were created by aligning multiple 13 × 25 μm-wide rectangular ROIs, each with a slightly different laser intensity (scale bar, 100 μm). **e**, Enzyme-mediated localized tethering of engineered $VEGF_{121}$ visualized by immunostaining. The right panel shows the background signal for the negative control conditions corresponding to FXIIIa-mediated crosslinking in the absence of $VEGF_{121}$. Scale bars, 200 μm. **f**, ProteinA tethering results in patterns of Fc-chimaeric proteins (here: IgG), in contrast to the control gel condition without ProteinA (right panel). Scale bars, 200 μm.

$VEGF_{121}$ resulted in 4.93 ng ml^{-1} (0.31 nM or 24.6% of total amount) of immobilized $VEGF_{121}$ in these gels (Supplementary Fig. S11). Furthermore, confocal microscopy imaging of fluorescent $VEGF_{121}$ revealed a relatively rapid decrease of the protein intensity within increasing penetration depth to circa 500 μm (Supplementary Fig. S12), suggesting that enzyme diffusion is the limiting parameter for protein coupling. Assuming a linear correlation of the $VEGF_{121}$ concentration with fluorescent intensity, we calculated the concentration profile across the entire thickness of the gel (Supplementary Fig. S13). On the basis of this profile and the total amount of incorporated $VEGF_{121}$ determined by enzyme-linked immunosorbent assay, we obtain for the given initial concentration in the labelling solution a maximal concentration of 0.26 ng ml^{-1} (16.25 pM) of immobilized protein at the gel surface.

To broaden the applicability of our patterning platform to any type of signalling protein in a generic and more widely accessible fashion, we immobilized proteins in hydrogels through binding to ProteinA (and ProteinG, not shown; Fig. 3f). ProteinA contains five high-affinity binding sites ($K_a = 10^8$ per mole) for the Fc-region of human, mouse and rabbit immunoglobulins, and thus allows for easy, site-selective immobilization of Fc-tagged proteins[4], many of which are commercially available. To this end, we modified ProteinA with caged Q-peptides and enzymatically patterned it within hydrogels. Indeed, the spatially controlled distribution of ProteinA nicely translates into specific patterns of Fc-tagged proteins as exemplified here by binding of Alexa488-modified IgG (Fig. 3f, left panel). Importantly, in the absence of ProteinA, no IgG binding was observed (Fig. 3f, right panel).

Finally, we sought to exploit light-activated enzymatic gel patterning for manipulating the behaviour of live cells directly in culture. As a physiologically relevant model system, we chose to control the 3D invasion of human mesenchymal stem/progenitor cells (termed mesenchymal stem cells (MSCs) herein; Fig. 4). MSCs are well known to migrate towards inflamed sites in tissues and are considered as key components of the complex microenvironment contributing to cancer maintenance and dissemination[26]. To modulate *in situ* and in three dimensions the direction of MSC invasion, we patterned the fibronectin-derived adhesion peptide RGD, the recombinant fibronectin fragment FN_{9-10} (ref. 24), and platelet-derived growth factor B (here, PDGF-BB; ref. 27), each engineered to comprise a Q-peptide. These biomolecules were selected because they play a role during MSC invasion[28–30] and because our MSCs express high levels of receptors for these signals (not shown).

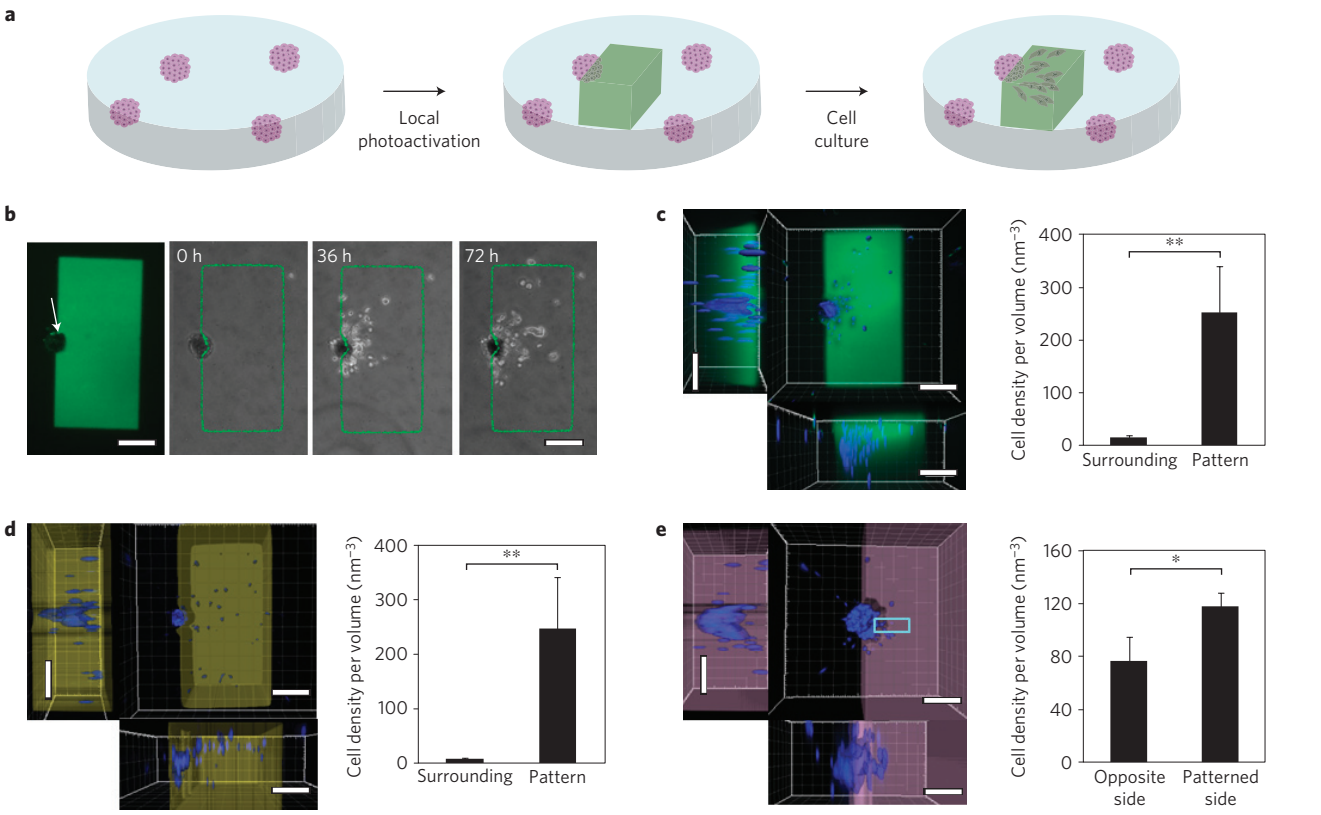

Figure 4 | *In situ* manipulation of 3D MSC invasion by light-activated enzymatic patterning. a, MSC microtissues are embedded in MMP-sensitive PEG hydrogels. *In situ* biomolecule patterning is used to direct MSC invasion in three dimensions. **b**, Confocal micrograph showing enzymatic patterning of the fluorescent adhesion peptide RGD in precisely defined cuboidal patterns (~900 × 450 μm) touching half of a microtissue (left panel, top view, microtissue indicated by arrow). MSCs rapidly invade the patterned gel regions as shown by time-lapse microscopy of one representative example (right panels). **c**, Confocal micrographs showing the 3D distribution of DAPI-stained MSC cell nuclei co-localized with the RGD pattern after 3 days in culture (left panel, top and side views; scale bars, 200 μm). Quantification reveals highly significant differences in cell densities inside and outside the RGD-patterned region (right panel; $^{**}p < 0.01$, error bars represent s.d., $n = 3$ independent experiments). **d**, Confocal micrographs showing the 3D distribution of DAPI-stained MSC cell nuclei within a gel locally patterned with FN_{9-10} (left panel, top and side views; scale bars, 200 μm). Quantification reveals highly significant differences in cell densities inside and outside the FN_{9-10}-patterned region (right panel; $^{**}p < 0.01$, error bars represent s.d., $n = 3$ independent experiments). **e**, 3D MSC invasion in a PDGF-patterned cell-adhesive PEG hydrogel. PDGF was immobilized in a smaller pattern next to the microtissue stained in blue (DAPI). The purple area indicates where migration due to PDGF activation is expected assuming radial outgrowth on MSC activation by PDGF (left panel; scale bars, 100 μm). Quantification reveals significant differences in cell densities caused by PDGF patterning (right panel; $^{*}p < 0.05$, error bars represent s.d., $n = 2$ independent experiments).

Multicellular clusters (microtissues) assembled from MSCs were incorporated into MMP-sensitive PEG hydrogels[23] bearing tethered caged K-peptide (Fig. 4a). On local uncaging of cuboidal patterns on one hemisphere of the microtissues, fluorescently labelled RGD and FN_{9-10} were enzymatically immobilized within gels, as shown for example in Fig. 4b. Strikingly, MSCs invade exclusively within patterned gel regions containing RGD (Fig. 4b,c and Supplementary Movie S1) or FN_{9-10} (Fig. 4d). In both cases, the differences between patterned and unpatterned regions are highly significant ($p < 0.01$) (Fig. 4c,d, right panels). Confocal imaging demonstrates invasion in three dimensions to a depth of approximately 300 μm (Fig. 4c,d, left panel), consistent with the $VEGF_{121}$ concentration profile determined above (Supplementary Fig. S13). Notably, the patterning of PDGF-BB in cell-adhesive and MMP-sensitive gels also resulted in significantly ($p < 0.05$) higher invasion in patterned regions (Fig. 4e). Therefore, light-activated enzymatic gel patterning can be exploited for manipulating the behaviour of live cells in three dimensions directly in culture.

Our experiments highlight that site-specific tethering of fragile proteins, such as adhesion proteins and growth factors, within gels by localized, laser-assisted uncaging is indeed feasible. Using a generic protein binding strategy, our method can be applied to virtually any kind of protein, and makes it a powerful alternative to selectively blocking the active site of biomolecules by photolabile groups[31,32]. The latter approach is straightforward for peptides but cumbersome in the case of full-length proteins. The automated *xyz*-positioning of the laser allows biomolecule patterning within gels with unprecedented flexibility and fidelity; the design of the patterns is indeed limited only by the user's imagination. We envision that this system could serve as a powerful tool in tissue engineering and cell biology to address questions related to spatiotemporal signalling of biomolecules such as morphogens. As one exciting example, the recapitulation of morphogen gradients within 3D structures and an investigation into their influence on the fate of developing pluripotent stem cells is conceivable.

Methods

Synthesis of caged peptide. Caged Fmoc-lysine (*N*α-Fmoc-*N*ε-Nvoc-lysine) (Supplementary Fig. S1) for standard Fmoc solid-phase peptide synthesis was synthesized following published protocols[33].

Photolysis reactions of caged peptide performed in solution. 100 μl of a 400 μM stock solution of caged K-peptide in water and 0.04% dimethylsulphoxide

(in a quartz cuvette) were exposed to the light of a Hg lamp (100 W) at a distance of 25 cm. Photocleavage of Nvoc was analysed by RP-HPLC coupled to mass spectrometry, revealing conversion to deprotected (uncaged) K-peptide with a different retention time and the expected loss in molecular mass (Supplementary Figs S2 and S3). To study the kinetics of photolysis, illumination was performed for different time points (0, 5, 8, 10, 15, 20 and 40 s) and assessed by analytical HPLC. Photolysis efficiency was determined on the basis of area ratios of peaks of the deprotected peptide [1] to the sum of caged peptide [1′] and deprotected peptide [1].

FXIIIa-mediated crosslinking in solution. FXIIIa was used at 1 U ml^{-1} for enzyme-catalysed crosslinking of the two substrates AcF**K**GGERCG-NH_2 (100 μM) and NQEQVSPLERCG-NH_2 (100 μM) in 100 μl of reaction buffer containing 50 mM $CaCl_2$, 50 mM Tris at pH 7.6 and 1 mM dithiothreitol. Reactions were conducted for 45 min at room temperature and stopped by the addition of 50 μl 0.1% trifluoroacetic acid in H_2O, and kept on ice before performing analytical RP-HPLC (C_{18}-column, Symmetry, Waters).

Preparation of thin PEG hydrogel films. PEG hydrogels (5% w/v) were prepared by Michael-type addition from two aqueous precursors containing 8arm-PEG–vinylsulphone and 4arm-PEG–thiol (ref. 34). Gelation was performed in 0.3 M HEPES at pH 7.9 at 37 °C for 20 min. Incorporation of 1 mM caged K-peptide through thiols of its cysteine residue rendered hydrogels photosensitive. Hydrogels were cast between 3-mercaptopropyl-trimethoxylsilane-treated glass slides and hydrophobic, siliconized glass slides (Sigmacote, SL-2) using 100 μm spacers. The obtained thin hydrogel layers were immersed in water to allow overnight swelling at 4 °C.

Laser-assisted hydrogel patterning. An upright point-scanning confocal microscope (Zeiss, 710 LSM) equipped with a 405 nm diode laser (30 mW) and with W N-Achroplan ×20/0.5 or EC Plan-Neofluar ×10/0.30 objectives was employed for local illumination of gels. The bleaching mode and user-defined ROI scanning option of the microscope software (ZEN2009) allowed precisely controlled arbitrary patterns in *xyz*. Precise control of specific laser intensities assigned to each ROI allowed the generation of biochemical gradients. For example, step-wise gradients were obtained by aligning seven contacting rectangular ROIs (100 μm width), each of which had assigned a different assigned laser intensity (100–80–60–40–20–10–5% of the maximal laser power). The time of laser irradiation was approximately 2.5 min, equal to the sum of 100 iterations of laser scanning. Continuous gradients were obtained by decreasing the laser power (18–5% of the maximal power) and by choosing smaller patterns (rectangles of 25 μm in width). In this case, the time of laser irradiation was approximately 1.5 min, equal to the sum of 200 iterations of laser scanning.

FXIIIa-mediated biomolecule tethering to hydrogels in two dimensions. Laser-treated hydrogels were immersed in FXIIIa-labelling solution (5 U ml^{-1} FXIIIa, 50 mM $CaCl_2$, 150 mM NaCl, and 50 mM Tris at pH 7.6) with a protein of interest bearing a FXIII substrate. To fluorescently visualize local FXIIIa-catalysed crosslinking, the Q-peptide was functionalized with a maleimide-functionalized Alexa Fluor dye (A-20347, Invitrogen) through its cysteine side chain thiol. FXIIIa-mediated fluorescent patterns were obtained on reaction with 150 μM fluorescent Q-peptide for 45 min at room temperature. The crosslinking reaction was stopped by adding washing buffer (100 mM NaCl and 50 mM Tris buffer, at pH 7.6). Fluorescent patterns were visible after about 30 min of washing, the time necessary for sufficient diffusion of non-bound fluorescent peptide. Fluorescent microscopy images were acquired after overnight washing at 4 °C to ensure complete diffusion of the soluble fluorescent peptide.

VEGF patterning. FXIIIa-catalysed patterning of a $VEGF_{121}$ variant comprising an exogenous Q-peptide was performed as described above. $VEGF_{121}$ (5.4 μg in 30 μl) of FXIIIa labelling solution was added to the laser-exposed hydrogels and left for 45 min at room temperature. After overnight washing in washing buffer at 4 °C, VEGF patterns were visualized by immunostaining with a VEGF-specific primary antibody (rabbit polyclonal VEGF, A-20, sc-152, Santa Cruz Biotechnology) followed by exposure to an Alexa Fluor 647 goat antirabbit secondary antibody (A-21245, Invitrogen). Fluorescent microscopy images were acquired after two hours of washing in PBS with 0.1% Tween.

ProteinA patterning. Gel modification by ProteinA was achieved in two steps comprising functionalization of ProteinA with maleimide groups by reacting it with a heterobifunctional PEG linker (NHS–PEG–maleimide, 5 molar excess), followed by attachment of the Q-peptide through its free thiol. The obtained Q-peptide-modified ProteinA (19.6 μg) was added to 30 μl FXIIIa reaction buffer for subsequent ProteinA immobilization on the laser-activated hydrogel. The reaction was conducted as described above. Control hydrogels were treated in the same manner except for the addition of ProteinA to FXIIIa reaction buffer. The patterns of tethered ProteinA were visualized by immunostaining with an Alexa Fluor 488 rabbit secondary antibody (A-11078, Invitrogen).

MSC culture and multicellular spheroid formation. MSCs previously isolated from human placenta[35] were cultured in DMEM with Glutamax supplemented with 1 mM sodium pyruvate, HEPES at pH 7.5, 5% penicillin/streptomycin and 10% fetal calf serum. Cells were used between passages 7 and 16. Multicellular spheroids were formed from 15×10^3 cells ml^{-1} using a hanging-drop technique (30 μl droplets) in serum-free DMEM with 20% methocel derived from methyl cellulose (Sigma) as described previously[36]. Spheroids were collected after overnight incubation and washed once in serum-free DMEM medium.

Preparation of PEG hydrogels for 3D cell culture. MMP-sensitive PEG hydrogels were formed as described previously[23] through Michael-type addition from two aqueous precursors containing 4arm-PEG–vinylsulphone (20 kDa) and the MMP substrate peptide GCRDGPQG↓IWGQDRCG (↓ indicates cleavage site, MW 1773 g mol^{-1}) at equimolar ratio and a final concentration of 3.4% (w/v). Gelation was performed in the presence of MSC spheroids in 0.1 M HEPES at pH 7.9 and 13% medium at 37 °C for 35 min. Caged K-peptide (1 mM) was incorporated in hydrogels. Gels (10 μl precursor solutions) were cast on μ-slide angiogenesis (ibidi, Germany). The obtained thin hydrogel layers were immersed in medium to swell to equilibrium at 37 °C.

FXIIIa-mediated biomolecule tethering to hydrogels in three dimensions. Laser-treated hydrogels were immersed for 90 min in FXIIIa-labelling solution (2 U ml^{-1} FXIIIa, 10 mM $CaCl_2$, 10 mM HEPES at pH 7.5 in serum-free DMEM medium) with peptides or recombinant proteins containing the exogenous FXIIIa substrate NQEQVSPL as a Q-peptide at the N terminus. The crosslinking reaction was stopped by washing with PBS followed by serum-free DMEM for several minutes. This procedure was repeated twice with subsequent overnight washing at 37 °C and 5% CO_2.

3D MSC invasion in patterned hydrogels. The Q-peptide-modified RGD peptide NQEQVSPL-RGDSPERCG was functionalized with a maleimide-functionalized Alexa Fluor 488 (A-10254, Invitrogen), and 150 μM of the peptide was added to the labelling solution and immobilized as described above. After overnight washing, hydrogels were immersed in DMEM supplemented with serum and 100 ng ml^{-1} recombinant human PDGF-BB (PreproTech) to stimulate cell migration. The same procedures were used for the recombinant fibronectin type III repeat 9–10 fragment (specifically referred to elsewhere as FNIII9*–10; ref. 24) (21 kDa, 130 μM) and a recombinant PDGF-BB variant (20 ng ml^{-1}) bearing exogenous Q-peptides (production described in Supplementary Information). In the latter case, hydrogels were rendered cell-adhesive by conjugating 30 μM RGD and were cultured in serum-free DMEM without PDGF supplement. Cells were fixed with 4% PFA, stained with 4′, 6-diamidino-2-phenylindole (DAPI) and visualized with confocal and bright-field microscopy. Quantification was performed using Fiji and Imaris software.

Received 1 March 2013; accepted 2 September 2013; published online 13 October 2013

References

1. Langer, R. & Tirrell, D. A. Designing materials for biology and medicine. *Nature* **428,** 487–492 (2004).
2. Lutolf, M. P. & Hubbell, J. A. Synthetic biomaterials as instructive extracellular microenvironments for morphogenesis in tissue engineering. *Nature Biotechnol.* **23,** 47–55 (2005).
3. Engler, A. J., Sen, S., Sweeney, H. L. & Discher, D. E. Matrix elasticity directs stem cell lineage specification. *Cell* **126,** 677–689 (2006).
4. Lutolf, M. P., Doyonnas, R., Havenstrite, K., Koleckar, K. & Blau, H. M. Perturbation of single hematopoietic stem cell fates in artificial niches. *Int. Biol.* **1,** 59–69 (2009).
5. Gilbert, P. M. *et al.* Substrate elasticity regulates skeletal muscle stem cell self-renewal in culture. *Science* **329,** 1078–1081 (2010).
6. Lee, K., Silva, E. A. & Mooney, D. J. Growth factor delivery-based tissue engineering: General approaches and a review of recent developments. *J. R. Soc. Inter.* **8,** 153–170 (2011).
7. Katz, J. S. & Burdick, J. A. Light-responsive biomaterials: Development and applications. *Macromol. Biosci.* **10,** 339–348 (2010).
8. Kloxin, A., Kasko, A. M., Salinas, C. N. & Anseth, K. Photodegradable hydrogels for dynamic tuning of physical and chemical properties. *Science* **324,** 59–63 (2009).
9. Wong, D. Y., Griffin, D. R., Reed, J. & Kasko, A. M. Photodegradable hydrogels to generate positive and negative features over multiple length scales. *Macromolecules* **43,** 2824–2831 (2010).
10. Ramanan, V. V. *et al.* Photocleavable side groups to spatially alter hydrogel properties and cellular interactions. *J. Mater. Chem.* **20,** 8920–8926 (2010).
11. Luo, Y. & Shoichet, M. S. A photolabile hydrogel for guided three-dimensional cell growth and migration. *Nature Mater.* **3,** 249–253 (2004).
12. Hahn, M., Miller, J. & West, J. Three-dimensional biochemical and biomechanical patterning of hydrogels for guiding cell behavior. *Adv. Mater.* **18,** 2679–2684 (2006).

13. Wosnick, J. H. & Shoichet, M. S. Three-dimensional chemical patterning of transparent hydrogels. *Chem. Mater.* **20,** 55–60 (2008).
14. DeForest, C. A., Polizzotti, B. D. & Anseth, K. S. Sequential click reactions for synthesizing and patterning three-dimensional cell microenvironments. *Nature Mater.* **8,** 659–664 (2009).
15. Wylie, R. G. *et al.* Spatially controlled simultaneous patterning of multiple growth factors in three-dimensional hydrogels. *Nature Mater.* **10,** 799–806 (2011).
16. Ellis-Davies, G. C. R. Caged compounds: Photorelease technology for control of cellular chemistry and physiology. *Nature Methods* **4,** 619–628 (2007).
17. Lorand, L. & Graham, R. M. Transglutaminases: Crosslinking enzymes with pleiotropic functions. *Nature Rev. Mol. Cell Biol.* **4,** 140–156 (2003).
18. Mosesson, M. W., Siebenlist, K. R. & Meh, D. A. The structure and biological features of fibrinogen and fibrin. *Fibrinogen* **936,** 11–30 (2001).
19. Sperinde, J. J. & Griffith, L. G. Synthesis and characterization of enzymatically-cross-linked poly(ethylene glycol) hydrogels. *Macromolecules* **30,** 5255–5264 (1997).
20. Hu, B. H. & Messersmith, P. B. Rational design of transglutaminase substrate peptides for rapid enzymatic formation of hydrogels. *J. Am. Chem. Soc.* **125,** 14298–14299 (2003).
21. Ehrbar, M. *et al.* Enzymatic formation of modular cell-instructive fibrin analogs for tissue engineering. *Biomaterials* **28,** 3856–3866 (2007).
22. Chan, B. P. Biomedical applications of photochemistry. *Tissue Eng. B* **16,** 509–522 (2010).
23. Lutolf, M. P. & Hubbell, J. A. Synthesis and physicochemical characterization of end-linked poly(ethylene glycol)-co-peptide hydrogels formed by Michael-type addition. *Biomacromolecules* **4,** 713–722 (2003).
24. Martino, M. M. *et al.* Controlling integrin specificity and stem cell differentiation in 2D and 3D environments through regulation of fibronectin domain stability. *Biomaterials* **30,** 1089–1097 (2009).
25. Ehrbar, M. *et al.* Cell-demanded liberation of VEGF(121) from fibrin implants induces local and controlled blood vessel growth. *Circ. Res.* **94,** 1124–1132 (2004).
26. Spaeth, E., Klopp, A., Dembinski, J., Andreeff, M. & Marini, F. Inflammation and tumor microenvironments: Defining the migratory itinerary of mesenchymal stem cells. *Gene Ther.* **15,** 730–738 (2008).
27. Martino, M. M. *et al.* Engineering the growth factor microenvironment with fibronectin domains to promote wound and bone tissue healing. *Sci. Transl. Med.* **3,** 100ra89 (2011).
28. Docheva, D., Popov, C., Mutschler, W. & Schieker, M. Human mesenchymal stem cells in contact with their environment: Surface characteristics and the integrin system. *J. Cell Mol. Med.* **11,** 21–38 (2007).
29. Tokunaga, A. *et al.* PDGF receptor beta is a potent regulator of mesenchymal stromal cell function. *J. Bone Miner. Res.* **23,** 1519–1528 (2008).
30. Veevers-Lowe, J., Ball, S. G., Shuttleworth, A. & Kielty, C. M. Mesenchymal stem cell migration is regulated by fibronectin through α5β1-integrin-mediated activation of PDGFR-β and potentiation of growth factor signals. *J. Cell Sci.* **124,** 1288–1300 (2011).
31. Ohmuro-Matsuyama, Y. & Tatsu, Y. Photocontrolled cell adhesion on a surface functionalized with a caged arginine-glycine-aspartate peptide. *Angew. Chem. Int. Ed.* **47,** 7527–7529 (2008).
32. Miller, D. S., Chirayil, S., Ball, H. L. & Luebke, K. J. Manipulating cell migration and proliferation with a light-activated polypeptide. *ChemBioChem* **10,** 577–584 (2009).
33. Rusiecki, V. K. & Warne, S. A. Synthesis of *N*-α-Fmoc-*N*-ε-Nvoc-lysine and use in the preparation of selectively functionalized peptides. *Bioorg. Med. Chem. Lett.* **3,** 707–710 (1993).
34. Cordey, M., Limacher, M., Kobel, S., Taylor, V. & Lutolf, M. P. Enhancing the reliability and throughput of neurosphere culture on hydrogel microwell arrays. *Stem Cells* **26,** 2586–2594 (2008).
35. Semenov, O. V. *et al.* Multipotent mesenchymal stem cells from human placenta: Critical parameters for isolation and maintenance of stemness after isolation. *Am. J. Obstet. Gynecol.* **202,** 193.e1–193.e13 (2010).
36. Korff, T. & Augustin, H. G. Integration of endothelial cells in multicellular spheroids prevents apoptosis and induces differentiation. *J. Cell. Biol.* **143,** 1341–1352 (1998).

Acknowledgements

We thank A. Negro for help with data analysis, A. Ranga, S. Allazetta, N. Brandenberg, Y. Okawa, K. Krishnamani, P. Abdel-Sayed and N. Balashubrmaniam for valuable discussion, C. Dessibourg, P. Briquez and the Protein Expression Core Facility of EPFL for assistance with recombinant protein production, A. Seitz and T. Laroche for support with confocal microscopy, R. Guiet and O. Burri for assistance with image processing, and S. Banala for sharing his experience with photocaging systems. This work was financially supported in part by a European Young Investigator (EURYI) Award (PE002-117115/1) and an ERC starting grant to M.P.L.

Author contributions

M.P.L., K.A.M. and L.K. designed research, analysed data and wrote the paper; K.A.M. and L.K. performed research; A.J.v.d.V. contributed to synthesis, purification and analysis of caged molecules; M.M.M., P.S.L., J.A.H. and M.E. contributed new reagents/analytic tools. All authors gave input on the manuscript draft.

Additional information

Supplementary information is available in the online version of the paper. Reprints and permissions information is available online at www.nature.com/reprints. Correspondence and requests for materials should be addressed to M.P.L.

Competing financial interests

The authors declare no competing financial interests.